Said Nechad[1], Ali Khelil[1], Mohamed HadjMeliani[2], Larbi Loukarfi[1], Mohamed Braikia[1]*

THREE-DIMENSIONAL NUMERICAL INVESTIGATION ON SWIRLING JETS AND ELLIPTIC JETS WITH DIFFERENT ASPECT RATIO

TRODIMENZIONALNO NUMERIČKO ISTRAŽIVANJE VRTLOŽNOG I ELIPTIČNOG STRUJANJA SA RAZLIČITIM FAKTORIMA PRESEKA DIFUZORA

Originalni naučni rad / Original scientific paper
UDK /UDC: 532.525:532.517.4

Rad primljen / Paper received: 11.11.2018

Adresa autora / Author's address:
[1)] Control, Testing, Measurement and Mech. Simulation Lab., Hassiba Benbouali University of Chlef, Algeria
[*] email: khelila@yahoo.fr or a.khelil@univ-chlef.dz
[2)] Lab. Theoretical Physics and Material Physics, LPTPM, Dep. of Mechanics, Faculty of Science, Hassiba Benbouali University of Chlef, Algeria

Keywords
- elliptic jet
- swirling jet
- aspect ratio
- numerical simulation
- diffuser configuration

Ključne reči
- eliptično strujanje
- vrtložno strujanje
- faktor preseka difuzora
- numerička simulacija
- konfiguracija difuzora

Abstract

This paper deals with the three-dimensional numerical simulation of aerodynamic characteristics of turbulent jets issuing from two diffusers configuration with different geometries. The first diffuser configuration is an elliptical shape with different aspect ratios AR = a/b, where a and b are the diffuser height and width varied from 1, 2, 4 and 8, while the second diffuser configuration generates the swirling jet through a diffuser provided with 60° inclined vanes. The comparison of the numerical results of the swirling jet and those of the elliptical jets, keeping the same equivalent diameter of the diffusers and the same flow conditions to the ambient environment, has been discussed. The numerical simulation is performed using two turbulences model, the standard k-ε model and the Reynolds stress model (RSM). The finite volume method with an unstructured tetrahedral mesh type has been used in this investigation. In the light of the results, we find that the swirling jet provides an improved flow mixing with large transversal velocities spreading in all sections of the resultant jet, compared to all studied elliptic jets.

Izvod

U radu je prikazana trodimenzionalna numerička simulacija aerodinamičkih karakteristika turbulentnog strujanja, koje nastaje iz dve konfiguracije difuzora, različitih geometrija. Prva konfiguracija difuzora je eliptičnog oblika, različitih faktora preseka AR = a/b, gde se a i b, visina i širina difuzora, menjaju u rasponu 1, 2, 4 i 8, dok se kod druge konfiguracije difuzora generiše vrtložno strujanje kroz difuzor snabdeven kanalima pod nagibom od 60°. Data je diskusija poređenja numeričkih rezultata vrtložnog i eliptičnog strujanja, sa nepromenjenim ekvivalentnim prečnikom difuzora i istim uslovima strujanja u odnosu na uslove okoline. Numerička simulacija je izvedena primenom dva turbulentna modela: standardnim k-ε i Rejnoldsovim naponskim modelom (RSM). Upotrebljena je metoda konačnih zapremina sa nestrukturnim tipom tetraedarske mreže. Na osnovu dobijenih rezultata, pronalazimo da vrtložno strujanje, u poređenju sa svim proučenim eliptičnim strujanjima, obezbeđuje poboljšano mešanje toka, sa većim poprečnim brzinama, koje se šire u svim presecima rezultujućeg mlaza.

INTRODUCTION

Flows involving the elliptic and swirling turbulent jets are encountered in a wide variety of industrial applications. The turbulent jets are applied in the technology of air conditioning systems, cooling and combustion, drying. The swirling jet promotes the mixing process, heat transfer and facilitates changes in the physical and chemical properties and the turbulence properties in the mean flow. Under the effect of swirling, the fluid particles tend to move away from the axis under the effect of centrifugal force. The main effect of turbulence is a dramatic increase in the spread in the fluid, that is to say exchanges of all kinds between the various parts of the flow. Turbulent diffusion leads to a very rapid homogenization of environments. Turbulent free jets have been the subject of several experimental and numerical researches in order to show the importance of the influence of turbulence and swirl to the flow studied. Most work on swirl jet are oriented to combustion chambers of engines, nuclear reactors and burners to obtain a homogeneous mixture of fuel and oxidizer /1, 2/. The swirling jet is particularly advantageous insofar as to incorporate the characteristics of the rotating flow. The nature of the blowing system, the diffuser disposition, the numbers of jets, the inclination of the vanes, the temperature of the blown air are the necessary parameters to achieve the swirl jet control as those studied by Braikia et al. /3/ and Khelil et al. /4, 5/. The elliptic jets have a large engineering practice and have general features between those of axisymmetric and plane jets. Lee and Baek /6/ showed that the effects of aspect ratio

on the characteristics of the turbulence of the elliptical jet were very important, especially the elliptical jet AR = 2. They showed vigorous turbulence characteristics in near the flow fields. The flow characteristics of elliptic jets are quite different from those of two-dimensional or axisymmetric jets and the entrainment rate of elliptic jets is several times greater than that of circular or plane jets They concluded that the jet spread along the minor axis is much greater than the along major axis. The jet cross section eventually switches its orientation at some distance downstream from the nozzle due to the difference in the spreading rate along the two symmetric axis planes. Quinn /7/ carried out measurements by hot wire anemometer on a turbulent free jet, isothermal and incompressible from a plate edged by elliptical orifice. The results show that the mixture in an elliptical jet from a sharp edge orifice plate is higher than the round jets and the jets issuing elliptical profiled nozzles. The jets issued from a rectangular and elliptical orifice with an aspect ratio AR = 2:1 have been studied by Imine et al. /8/. The second order model (RSM) was used by the author to simulate the flow field. They found that the asymmetric geometry substantially improved mixing in comparison with the axisymmetric case. Koseoglu and Baskayab /9/ investigate the differences between the impinging, round and elliptical jets, in terms of flow field and heat transfer characteristics. They found that the differences are reduced with increasing distance from the jet plate. Kuznik et al. /10/ have tested four two-equations turbulence models: a k-ε realizable model, a k-ε RNG model, a k-ω model and a k-ω SST model. They found that although the models can reasonably predict the cases of hot jet and isothermal jet, but fail for the cold jets. Based on the work carried out by Kuznik et al. /11/ they suggested that the turbulence model for second order quadratic RSM would be more appropriate for simulating ventilated enclosures with thermal effects. The effect of various parameters on the development of flow behind a vane diffuser has been studied experimentally and numerically by Raj Thundil and Ganesan, /12/. This work has highlighted the main features of the flow field generated by the diffuser with inclined vanes. The originality of this study is to arrive at the best angle vane using appropriate turbulence models both weak and strong swirl. They found that for weak swirl, the standard k-ε model is sufficient, while for strong swirl, the Reynolds stress model (RSM) is more appropriate. Ahmadvand et al. /13/ experimentally and numerically studied the influence of axial vane diffuser on increasing the heat transfer and turbulent fluid flow. Their study was conducted for three vane angles of 30°, 45° and 60° with uniform conditions of heat flow with the air that is used as working fluid. These authors have confirmed that the use of blades for generating swirling jet leads to improving heat transfer compared to those obtained from tubes without blades. They also found that the thermal efficiency increases when the blade angle is high and decreases by the growth of the Reynolds number. Escue and Cui /14/ presented a numerical study of a swirling flow to the inside of a straight pipe. Calculations are performed using a commercial software *Fluent*. The turbulence models used in this study include the RNG k-ε and Reynolds stress model (RSM). They found that the model RSM is most appropriate when the swirling flow is increased. Castro and Demuren /15/ investigated numerically using large eddy simulation of a turbulent rotating pipe flow and swirling jet flow, emitted from the pipe, into open quiescent ambient. In this study, various rotation rates and Reynolds numbers have been used. The simulations are performed with two kinds of swirl numbers (S = 0 and S = 0.5). The computations are realized with the FLUENT code. They observed that the swirl changes the characteristics of the jet flow field, leading to increased jet spread and axial velocity decay. For this study, we are interested in the influence of the geometry of the diffuser, on an isothermal turbulent free-jet structure. The numerical simulation is based on a light gas such as air, which comes out of a conical elliptical orifice with different aspect ratios and a swirl generator with vanes inclined by a 60° angle, keeping the same hydraulic diameter for the diffuser, and the same transmission conditions, to the environment. In the remainder of this paper, we present a literature investigation on swirling and elliptic jets and setting out the main results established in section 1. In section 2, we describe the computational domain. In section 3, we briefly review turbulence modelling and the governing equations. In section 4, we present the numerical results and some validations and discussions. Finally, in section 5, we give a summary of our conclusions.

PROBLEM DESCRIPTION AND COMPUTATIONAL DOMAIN

The free jet type flow through a conical elliptical opening with different aspect ratios (AR) and swirling jet is strongly influenced by the effects of changing the geometry of the diffuser. The computational domain considered in our work is in two volumes, so it is fully consolidated into a single volume (Fig. 1). The first volume is characterized by two types of configuration. The first one is an elliptical diffuser shape with different aspect ratios AR = a/b, where a and b are the nozzle height and width, varied from 1, 2, 4 and 8 (see Fig. 1 A, B, C and D) and the second one is a swirling diffuser with 14 inclined vanes by 60° (see Fig. 1 E). The first volume is characterized by a jet of air exiting from the diffuser at a velocity U =10 m/s, giving a Reynolds number based on the equivalent diameter of 4.10^4 to the surroundings, which is considered a second circular volume (Lee and Beak, /6/). The second volume is characterized by a diameter D = 400 mm, and a length along the axis of flow (X), which is equal to 1000 mm. The orifices investigated in this paper have the same equivalent diameter (D_e), equal to 60 mm, and a thickness of elliptical orifice 4 mm. For more detailed information concerning the orifice geometry, see Table 1 and Fig. 1.

Table 1. A conical elliptical orifice size and swirler diffuser.

Type of diffuser	AR	a (mm)	b (mm)
Swirler	1	30.0	30.0
Elliptical	1	30.0	30.0
	2	42.4	21.2
	4	60.0	15.0
	8	84.9	10.6

This work deals with numerical simulation of three-dimensional isothermal turbulent free jet, blowing from different diffuser geometry configuration. The analysis of the turbulent flow is to determine the mean dimensionless velocity fields, dimensionless Reynolds shear stress profiles and turbulence kinetic energy profiles along the major (*XZ*) and minor (*XY*) planes at cross-sections of X/D_e = 2, 3, 5 and 7 for different aspect ratio AR (a/b = 1, 2, 4 and 8) and swirling jet. The computation is performed using the finite volume method. The k-ε model and the Reynolds stress turbulence model (RSM) is used for closing the system of equations. The numerical calculations have been carried out in three dimensions, for any geometry of the elliptical diffuser and swirl diffuser. The numerical prediction was performed with the following assumptions: The flow is steady and isothermal. PRESTO and SIMPLE algorithm were used respectively for the interpolation of the pressure and the pressure coupling with the velocity; the pressure is set to 101 000 Pa (1 atm). To capture these effects, the mesh must meet certain requirements. Then, the simulation requires a careful choice of different parameters of the calculation code. The adopted mesh is an unstructured tetrahedral grid. Figure 2 shows the geometry and the mesh size of the swirl diffuser (Fig. 2a) and an elliptic diffuser with aspect ratios AR = 1 (see Fig. 2b). The type of mesh used allowed us to generate a number of nodes, of about 2 790 648 for different geometries. For our three-dimensional study, the cell surfaces are not necessarily of regular form. To calculate the volume of the cells and the surface of their faces, appropriate approximations are necessary. The simplest method is to represent the face of the cell by a series of triangular planes as in Fig. 2.

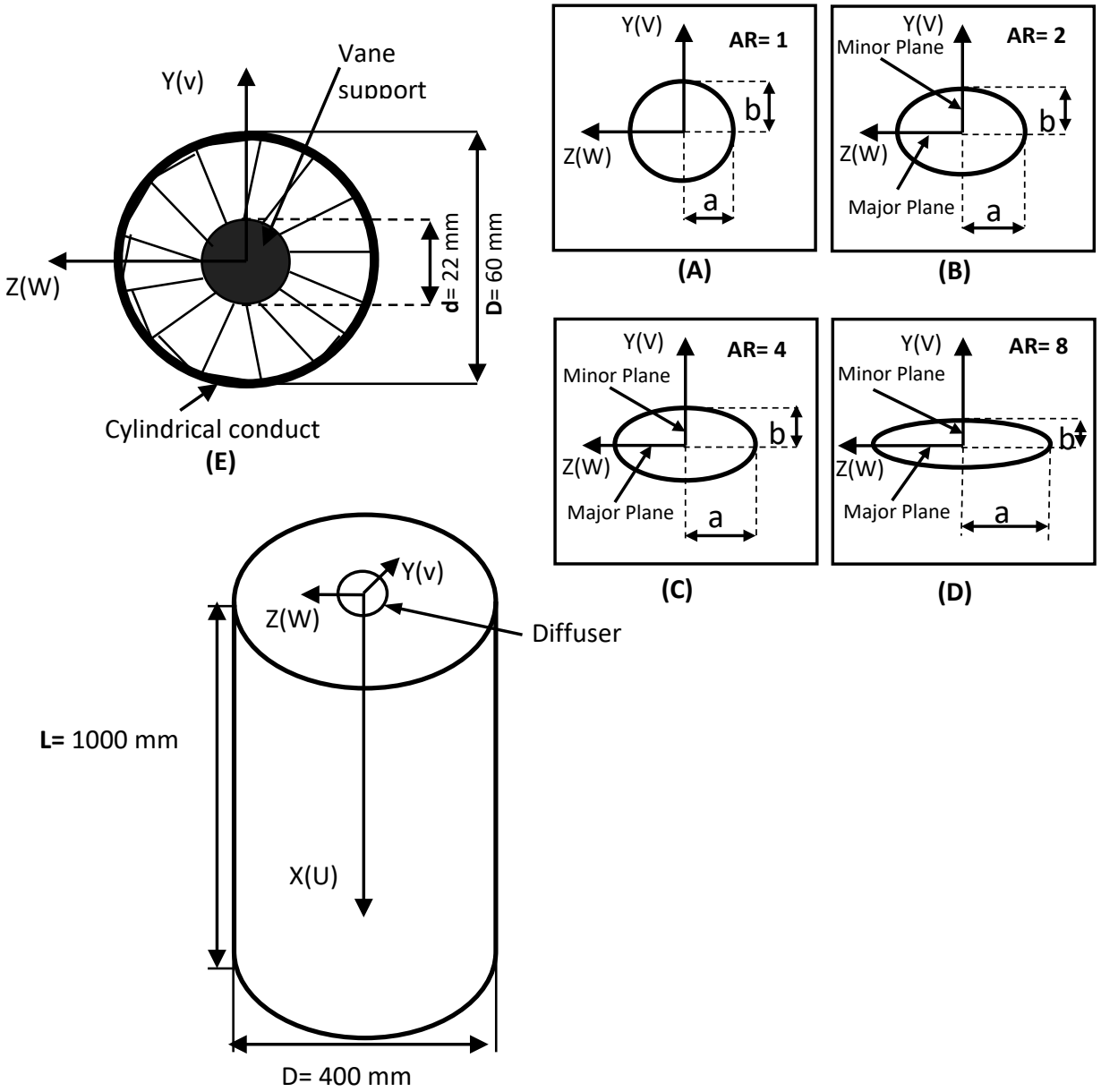

Figure1. Computational domain: (A, B, C and D) elliptical jet diffuser with aspect ratio (AR = 1, 2, 4 and 8), and (E) swirl diffuser.

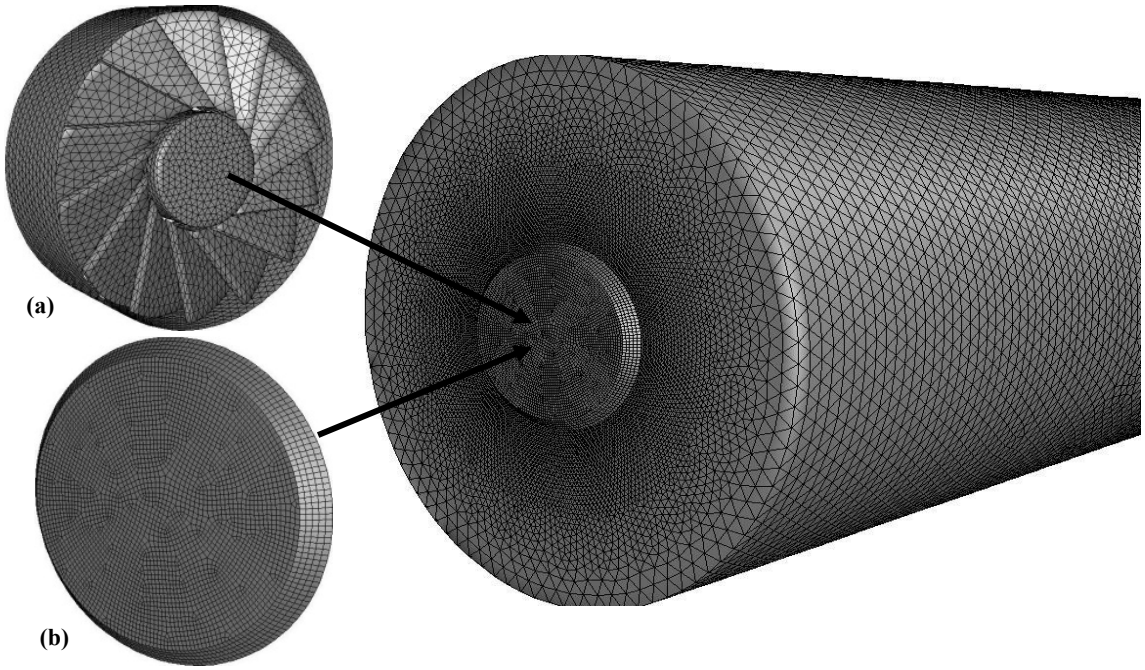

Figure 2. Computational domain of diffuser configurations and schematic grid used for: (a) swirl generator, (b) elliptical jet, AR = 1.

Calculations on different meshes (see Fig. 3) show that the transversal velocity of the solution does not change significantly. We can therefore conclude that the solution is independent of the mesh.

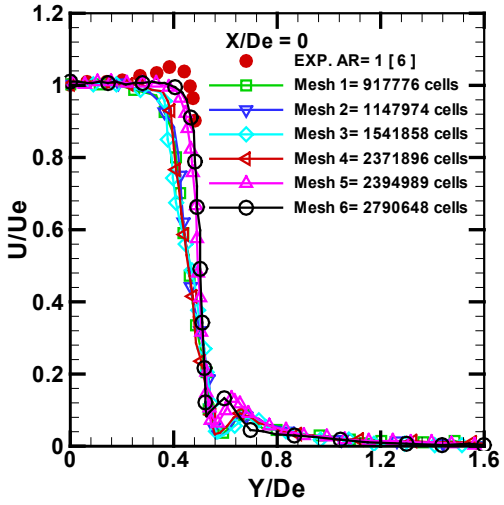

Figure 3. Independence of the meshing in elliptic jet case AR = 1.

NUMERICAL SIMULATION

Turbulence model

For a steady flow, three-dimensional, incompressible, and turbulent and with the constant properties of the fluid, the equations governing the flow are the conservation of mass and momentum equation written in Cartesian tensor notation as follows:

$$\frac{\partial U_i}{\partial x_i} = 0\,, \tag{1}$$

$$\rho \frac{\partial (U_i U_j)}{\partial x_j} = -\frac{\partial P}{\partial x_i} + \frac{\partial}{\partial x_j}\left[\mu\left(\frac{\partial U_i}{\partial x_j} + \frac{\partial U_j}{\partial x_i}\right) - \overline{\rho u_i' u_j'}\right]. \tag{2}$$

where: U_i is the average velocity; u'_i, u'_j are the corresponding fluctuation components; $-\overline{\rho u_i' u_j'}$ are average Reynolds stresses that must be modelled to close the equations. Note that here, temperature fluctuations are negligible and the Mach number is low (< 0.3), which allows us to assume that the fluid is incompressible (constant density).

The k-ε turbulence model is an example of two equations using the assumption of Boussinesq. Here, two closure turbulent models: Reynolds stress (RSM) and standard k-ε are used. Turbulence models with two equations (k-ε or other) provide good predictions on the physical characteristics of flow giving most industrial interest. In the flows where turbulent transport or non-equilibrium effects are important, the Boussinesq assumption is no longer valid and results of the hypothesis of Boussinesq model may be inaccurate. The Reynolds stresses model shows greater predictive performance with respect to the Boussinesq hypothesis because of isotropic nature. Therefore, the complete transport anisotropic models such as Reynolds stress (RSM) are necessary for accurate prediction for the swirling turbulent flow. In RSM, the Reynolds stresses are calculated directly, where different terms from left to right are, in respect: convection, diffusion, production, pressure, viscous dissipation and an additional production term. Note that the terms of convection and production are accurate, while the remaining terms are to be modelled /16, 17/. Detailed derivations for closure equations can be found in FLUENT 6.3 /18, 19/,

$$\underbrace{\frac{\partial}{\partial x_k}\left(\rho u_k \overline{u_i' u_j'}\right)}_{\text{convection}} - \underbrace{\frac{\partial}{\partial x_k}\left(\mu \frac{\partial}{\partial x_k}\overline{u_i' u_j'}\right)}_{\text{molecular diffusion}} =$$

$$= \underbrace{D_{T,ij}}_{\text{turbulent diffusion}} + \underbrace{P_{ij}}_{\text{production}} + \underbrace{\Phi_{ij}}_{\text{pressure strain}} + \underbrace{\varepsilon_{ij}}_{\text{dissipation}} + \underbrace{F_{ij}}_{\text{production by system rotation}} \tag{3}$$

BOUNDARY CONDITIONS

The boundary conditions used in this study are of 3 types called by convenience: inlet velocity, pressure outlet and wall. Inlet type conditions are used in the case of a flow entering within the field. The conditions wall type boundary, are assigned to impermeable walls flow, finally, if the flow is in contact with the outside, using the conditions of pressure outlet. Provided at the input (considered for the first volume). Generally, in the simulation of flows, the air entry profile is deduced from experimental data /3-6/. The operating conditions are reported in Table 2.

Table 2. Operating conditions.

Parameters	Elliptical and swirl diffuser
Reynolds number	$4 \cdot 10^4$
Hydraulic diameter	0.06 m
Turbulence intensity	7 %
Under relaxation	pressure = 0.3, density = 0.8 other parameters = 0.5
Convergence criteria	all parameters = 10^{-3}
Inlet velocity	10 m·s^{-1}
Pressure	101000 Pa
Walls	no-slip conditions
Outlet	pressure outlet

RESULTS AND DISCUSSION

The mean velocity profiles along *XY* (minor axis) plane and *XZ* (major axis) plane at cross-sections of X/D_e = 2, 3, 5 and 7 for different aspect ratio AR (a/b = 1, 2, 4, 8) are given in Figs. 4 to 6, respectively. The numerical prediction is performed by two turbulence models (standard k-ε and RSM). Along the major plane, the shear layer shrinks into the jet centre, while along the minor plane, the shear layer spreads out widely into the ambient fluid. In the case of AR = 8, the velocity profile along the major plane at X/D_e = 2 shows a nearly flat hump shape. The breakdown process through which the slender elliptic swirling structure is divided into substructures may cause this. Moreover, we note that the standard k-ε model does not correctly reproduce the experimental results. This result is expected, given the nature of the model. The Reynolds stress model improves the prediction of this quantity. As can been seen, the predictions of transversal dimensionless velocity profiles using the Reynolds stress model are in generally good agreement with the experimental data. Both models underestimate the amplitude of the velocity at the centreline at AR = 8 in all stations, as seen in Fig. 6.

Figure 7 shows a comparison of numerical results of the swirling jet to elliptical jets obtained for dimensionless velocities based on the turbulence model RSM for stations X/D_e = 2, 3, 5 and 7. Noting that in the case of the elliptical jet with AR = 1 and swirling jet, the major plane is equal to the minor plane ($a = b$). We can distinguish broadly a difference between the two cases. For swirling jet, we have in the plane *XY* (minor axis) and plane *XZ* (major axis) of the peak values, similar to each station with a sinusoidal distribution, where there is a decrease in velocity amplitude, due to the existence of internal recirculation zones, as can be seen in Fig. 7. It is also noted that the peaks are higher when axially approaching from the blow diffuser. While moving

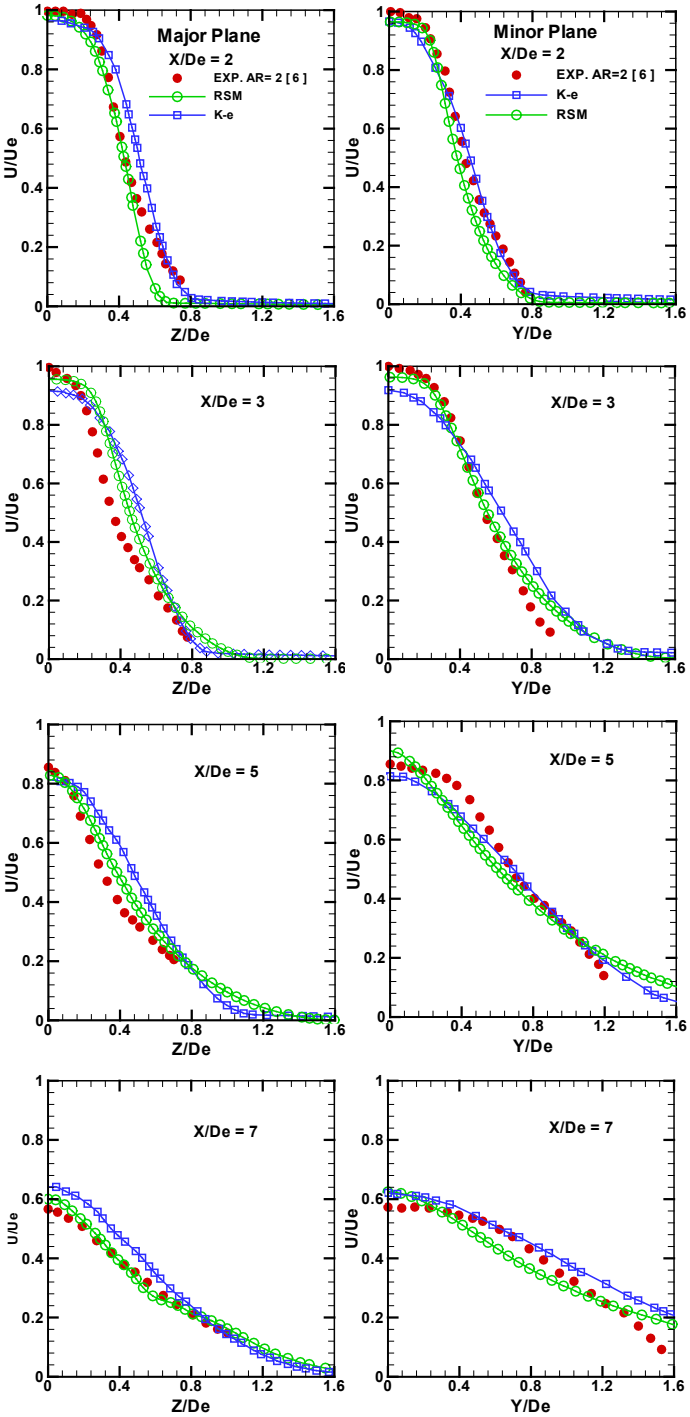

Figure 4. Velocity profiles U/U_e of elliptical jet with aspect ratio AR = 2 along *XY* (minor axis) plane and XZ (major axis) plane determined by the K-ε standard and RSM turbulence models at stations (X/D_e = 2, 3, 5 and 7).

downstream from the blowing orifice and jet centreline, it is observed that the velocity decreases to zero. As can be contested, the dimensionless velocity profiles move from the high values, decrease and then finally approach asymptotic value which refers to the outlet conditions. Therefore, it can be deduced that the flow spreads in the transversal direction. For elliptic jets, we notice that flow velocity profiles are uniform with gaps between them to each station. We also note that a reduction in average velocity, while

increasing the aspect ratio (AR), yields slower velocity values at station X/D_e = 2; 3; 5 and 7 in both planes, this remark is clearly shown in Fig. 7. Noting that for all stations in the major and minor planes, the swirl jet gives a large spread in the transversal direction compared to the elliptical jet with all different aspect ratios.

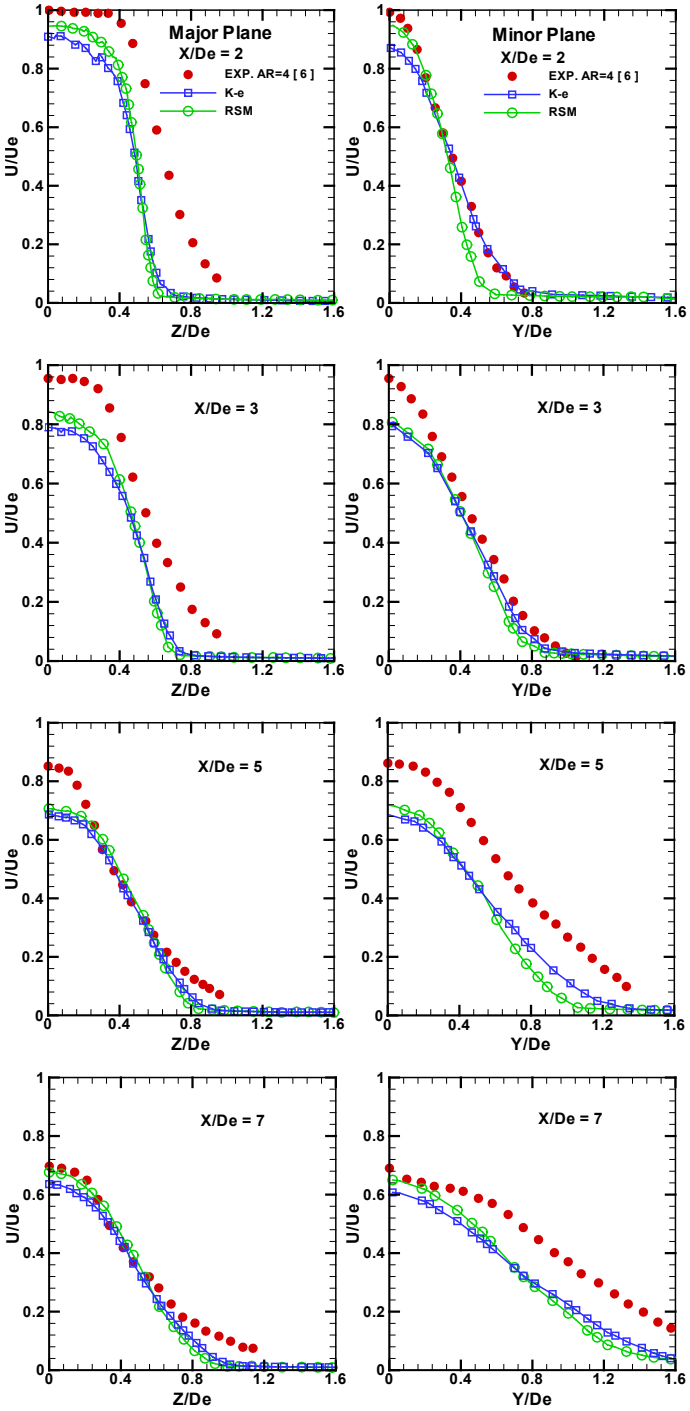

Figure 5. Velocity profiles U/U_e of elliptical jet with aspect ratio AR = 4 along XY (minor axis) plane and XZ (major axis) plane determined by the K-ε standard and RSM turbulence models at stations (X/D_e =2, 3, 5 and 7).

The turbulent kinetic energy distributions along major and minor axis at each cross-section (X/D_e = 2, 3, 5 and 7) for different configuration of elliptic jet and for swirling jet are shown in Fig. 8. At X/D_e = 2, the turbulent kinetic energy (q^2) of an elliptic jet with AR = 8 and swirling jet have distinct values compared to other elliptic jet configurations. Due to the largest turbulence intensity and kinetic energy, values generated from strong turbulence activities occurring near the blowing diffuser and thus the turbulence intensity and kinetic energy reach a maximal value. Far from downstream, turbulence fluctuations gradually decrease and attain the state of isotropic turbulence. The turbulent

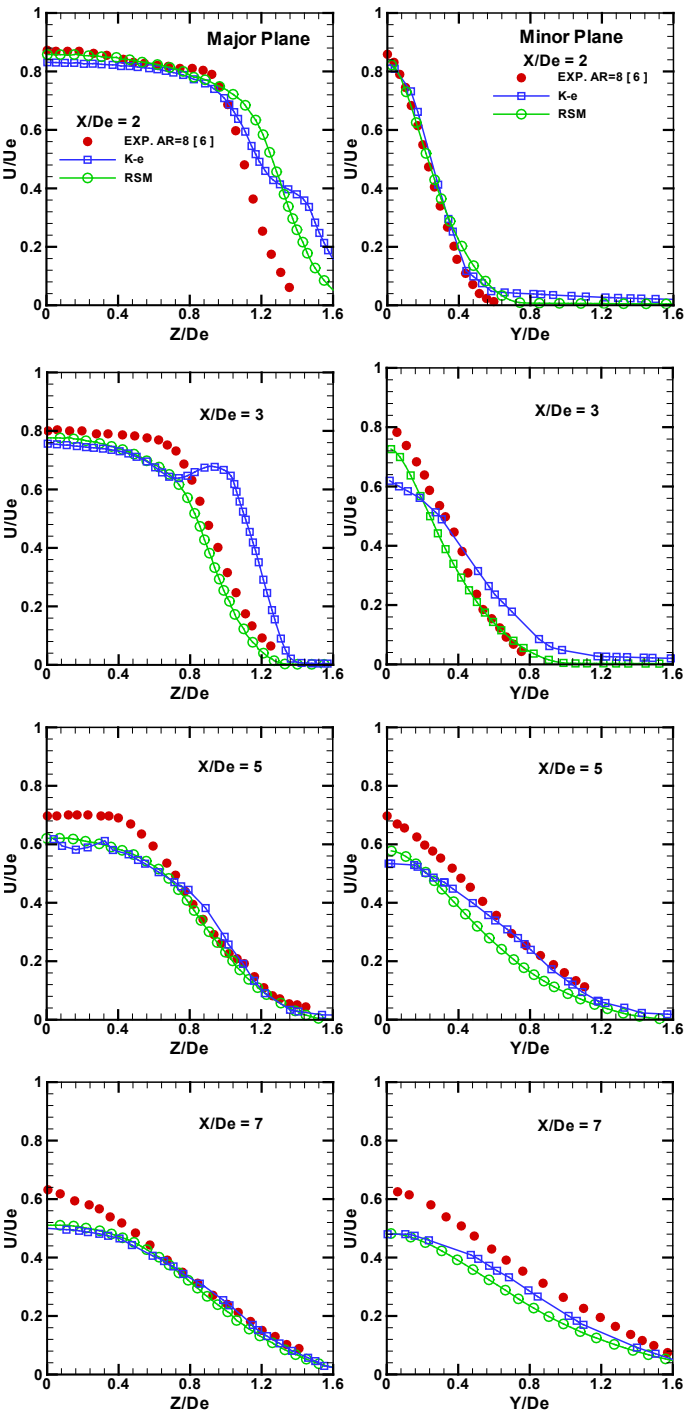

Figure 6. Velocity profiles U/U_e of elliptical jet with aspect ratio AR = 8 along XY (minor axis) plane and XZ (major axis) plane determined by the K-ε standard and RSM turbulence models at stations (X/D_e =2, 3, 5 and 7).

kinetic energy distributions q^2 in the minor plane have a higher value than in the major plane for the elliptic jet but the swirl jet preserves the same values in both planes. In particular, the turbulent kinetic energy has large values at $X/D_e = 5$ for AR = 2 and at $X/D_e = 7$ for AR = 4. The location of the peak value of q^2 moves to the centreline of the flow and the peak of swirling jet moves to the transversal direction giving a large spreading. The swirling jet has strong turbulence characteristics and good mixing and entrainment effects compared to elliptic jets.

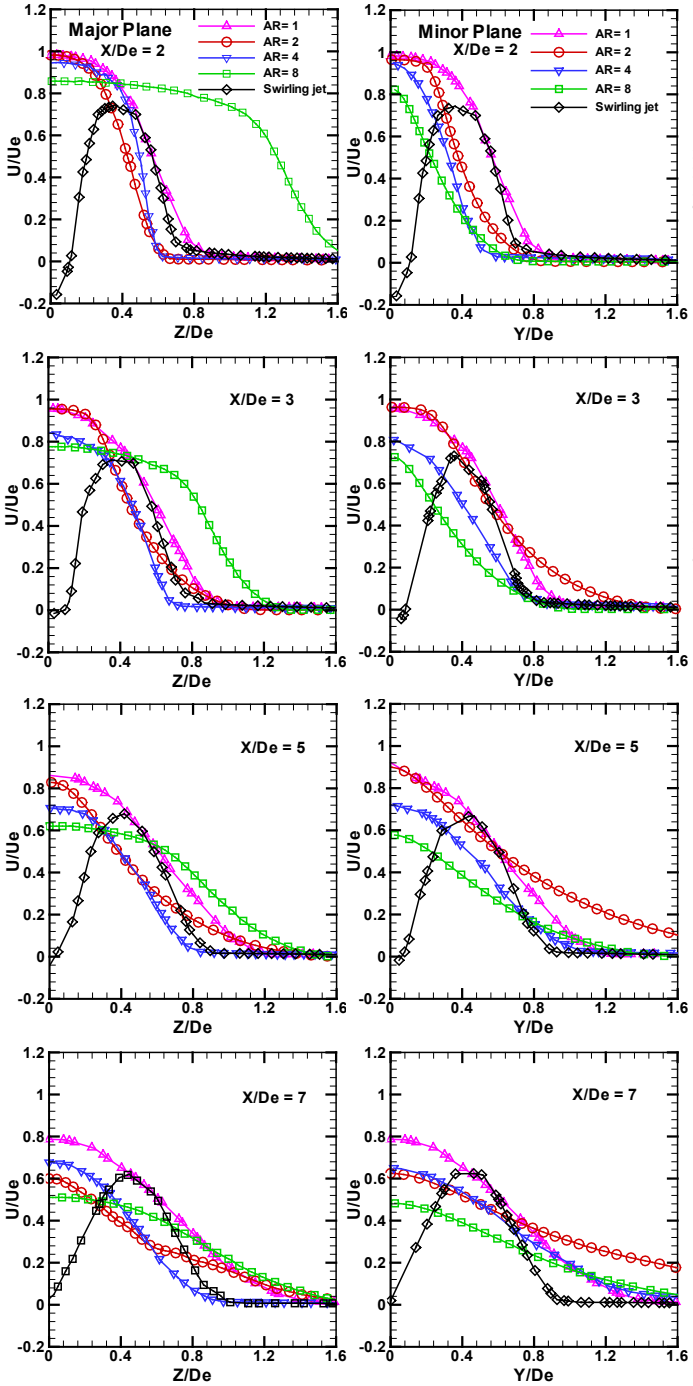

Figure 7. Velocity profiles U/U_e of swirling jets and elliptical jets with aspect ratio AR = 1, 2, 4 and 8 along *XY* (minor axis) plane and *XZ* (major axis) plane determined by the RSM turbulence model at stations (X/D_e = 2, 3, 5 and 7).

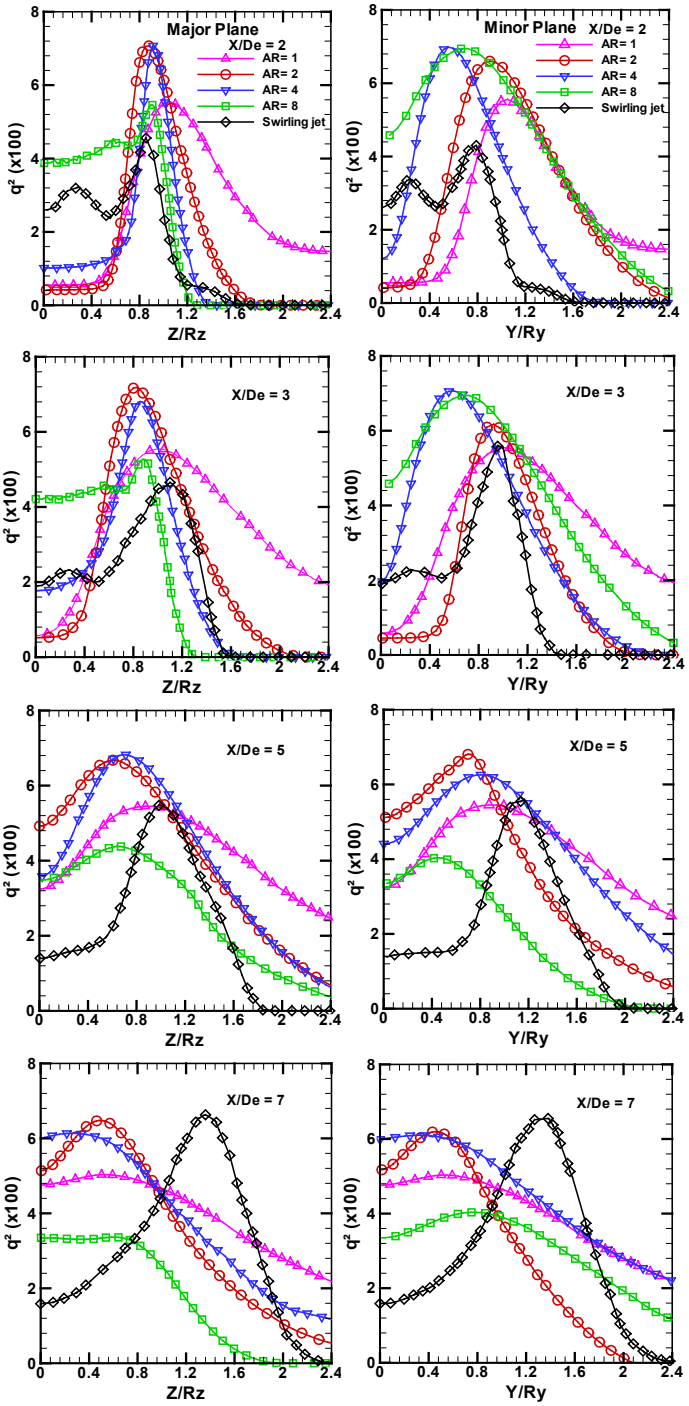

Figure 8. Turbulence kinetic energy profiles of swirling jets and elliptical jet with aspect ratio AR = 1, 2, 4 and 8 along *XY* (minor axis) plane and *XZ* (major axis) plane determined by the RSM turbulence model at stations (X/D_e = 2, 3, 5 and 7).

Reynolds shear stress profiles, R_{uw} in the major plane, and R_{uv} in the minor plane, are shown in Fig. 9. The dimensionless Reynolds shear stress R_{uw} and R_{uv} are defined by $\overline{uw}/U_e^2$ and $\overline{uv}/U_e^2$ respectively. For the different elliptic jets, the Reynolds shear stress profiles R_{uw} and R_{uv} have a peak value near $Y/R_y = 1$, on the other hand for the swirling jet, R_{uw} and R_{uv} have a peak value near $Y/R_y = 1.6$. This implies that most of the turbulent kinetic energy is produced by the non-organised random motion near the dif-

fuser at the centreline of the flow for different configuration of elliptic jet and far from the diffuser in transversal direction for the swirling jet. From this, we can see that the energy production of turbulence is more vigorous in the swirling jet compared to elliptic jets.

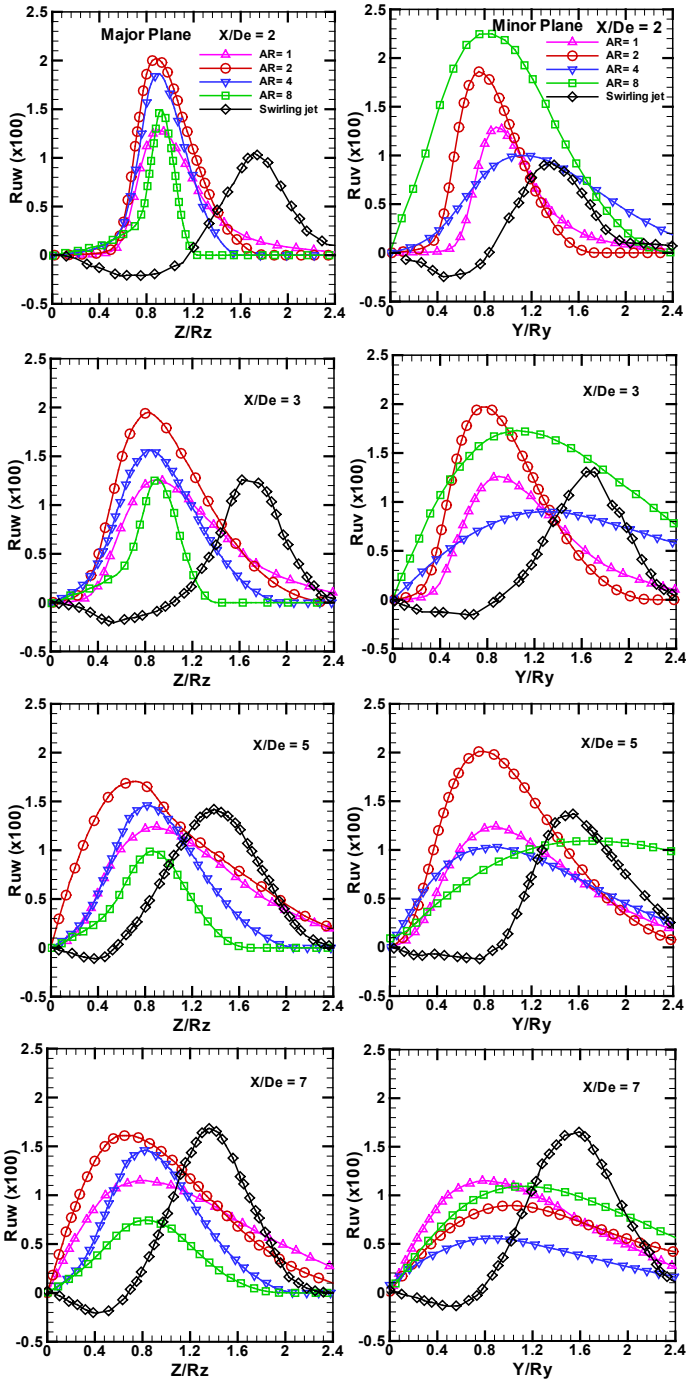

Figure 9. Reynolds shear stress profiles of swirling jets and elliptical jets with aspect ratio AR = 1, 2, 4 and 8 along *XY* (minor axis) plane and *XZ* (major axis) plane determined by the RSM turbulence model at stations (X/D_e = 2, 3, 5 and 7).

CONCLUSION

The objective of this investigation is to numerically simulate three-dimensional aerodynamics of the swirling and elliptic free jets. In this study, the jet is assumed isothermal. Two types of diffuser configurations are tested. The first diffuser configuration is elliptic with different aspect ratios (AR = 1, 2, 4 and 8) and the second configuration of the diffuser is a swirler with 14 vanes inclined at 60°, keeping the same equivalent diameter.

From a technological point of view, these types of jets are applied in air-conditioning and ventilation devices, hence the importance of having a good mix, and increased transversal spreading. In particular, this study is based on the analysis of velocity fields in free flow, which is highly dependent on the geometric orifice conditions. Thus, based on experimental results and numerical simulations obtained, we can draw the following conclusions: the experimental study shows that the characteristics of turbulent flow of elliptic jets with four different aspect ratios are quite different compared to those of round and swirling jet. In the region near the blow diffuser, the elliptical jets show a training force, and a higher mixing than round jets. In particular, elliptical jet AR = 2 have higher average speed amplitudes. Thus, elliptical jets, with aspect ratio AR = 2, can effectively use such devices in ventilation and drying systems. A comparison between the numerical results of the swirling jet to the elliptic jets is presented to determine the best configuration of the airflow jet. These results clearly show that the swirling jet induces an internal recirculation zone observed by a decrease in velocity located at the centreline. It is found that the influence of the geometry of the diffuser on the jet is fundamental. The swirl jet ensures dynamic homogenizing improved mixture with a large transversal spreading, which can be used in a large space. The swirling jet is an appropriate way to improve the quality of homogenization. Compared to all of the investigated elliptic jets, the swirl jet ensures improved mixing with a significant development of the transversal velocity in all sections of the resultant jet.

NOMENCLATURE

Latin symbols

a	major axis radius of the elliptic nozzle
b	minor axis radius of the elliptic nozzle
AR	aspect ratio of the nozzle ($\equiv a/b$)
d	vane support diameter, (m)
D	inner diameter of swirling jet, (m)
D_e	equivalent diameter of elliptic nozzle ($\equiv 2(ab)^{1/2}$) (m)
P	pressure, (Pa)
q^2	turbulent kinetic energy ($\equiv \frac{1}{2}(\overline{U'^2}+\overline{V'^2}+\overline{W'^2})/U_e^2$)
R_{uv}	Reynolds shear stress ($\equiv \overline{U'V'}/U_e^2$)
R_{uw}	Reynolds shear stress ($\equiv \overline{U'W'}/U_e^2$)
R_z, R_y	jet half-widths on major and minor planes, in respect
u'_i, u'_j	fluctuating velocity components, (m·s^{-1})
U', V', W'	fluctuating velocities in X, Y and Z directions, (m·s^{-1})
U_e	nozzle exit velocity in the X direction, (m·s^{-1})
U_i, U_j	average velocity components, (m·s^{-1})
X	coordinate in the jet axial direction
Y	coordinate in the jet minor axis plane
Z	coordinate in the jet major axis plane
$Z(W)$, $Y(V)$	axis of main velocity components along the major and minor planes, respectively
α	inclination angle of the vanes

Greek symbols

μ dynamic viscosity, ($kg \cdot m^{-1} \cdot s^{-1}$)
ρ air density, ($kg \cdot m^{-3}$)

Subscripts

e equivalent
i, j, k components indices

REFERENCES

1. Roudane, M., et al. (2013), *Numerical investigation of thermal characteristics of confined rotating multi-jet*, Mec. Ind., 14(4): 317-324. doi: 10.1051/meca/2013071
2. Khelil, A., et al. (2015), *Comparative investigation on heated swirling jets using experimental and numerical computations*, Heat Transfer Eng., 36(1): 43-57. doi: 10.1080/01457632.2014.906279
3. Braikia, M., et al. (2012), *Improvement of thermal homogenization using multiple swirling jets*, Therm. Sci., 16(1):237-248. doi: 10.2298/TSCI101026131B
4. Khelil, A., et al. (2009), *Prediction of high swirled natural gas diffusion flame using a PDF model*, Fuel, 88(2): 374-381. doi: 10.1016/j.fuel.2008.09.008
5. Khelil, A., et al. (2012), *Numerical study of the influence of combustion models and kinetic schemes when predicting the diffusion flames*, J Mech., 28(4): 701-713. doi: 10.1017/jmech.2012.108
6. Lee, S.J., Baek, S. (1994), *The effect of aspect ratio on the near-field turbulent structure of elliptic jet*, Flow Meas. Instrum., 5(3): 170-180. doi: 10.1016/0955-5986(94)90016-7
7. Quinn, W.R. (2007), *Experimental study of the near field and transition region of a free jet issuing from a sharp-edged elliptic orifice plate*, Eur. J Mech. B-Fluids, 4(26): 583-614. doi: 10.1016/j.euromechflu.2006.10.005
8. Imine, B., et al. (2006), *Study of non reactive isothermal turbulent asymmetric jet with variable density*, Comp. Mech., 38(2): 151-162.
9. Koseoglu, M.F., Baskayab, S. (2008), *The effect of flow field and turbulence on heat transfer characteristics of confined circular and elliptic impinging jets*, Int. J Therm. Sci., 47(10): 1332-1346. doi: 10.1016/j.ijthermalsci.2007.10.015
10. Kuznik, F., Rusaouen, G., Brau, J. (2007), *Experimental and numerical study of a full scale ventilated enclosure: Comparison of four two equations closure turbulence models*, Build. Environ., 42(3): 1043-1053. doi: 10.1016/j.buildenv.2005.11.024
11. Kuznik, F., Brau, J., Rusaouen, G. (2007), *A RSM model for the prediction of heat and mass transfer in a ventilated room*, Building Simulation, Beijing, China
12. Raj Thundil, K., Ganesan, V. (2008), *Study on the effect of various parameters on flow development behind vane swirlers*, Int. J Therm. Sci., 47(9): 1204-1225. doi: 10.1016/j.ijthermalsci.2007.10.019
13. Ahmadvand, M., Najafi, A.F., Shahidinejad, S. (2010), *An experimental study and CFD analysis towards heat transfer and fluid flow characteristics of decaying swirl pipe flow generated by axial vanes*, Meccanica, 45(1): 111-129.
14. Escue, A., Cui, J. (2010), *Comparison of turbulence models in simulation swirling pipe flows*, Appl. Math. Model., 34(10): 2840-2849. doi: 10.1016/j.apm.2009.12.018
15. Castro, N.D., Demuren, A.O. (2015), *Large eddy simulation of turbulent axially rotating pipe and swirling jet flows*, J Mech. Eng. Sci., 231(9):1749-1761. doi: 10.1177/0954406215620823
16. El Drainy, Y.A., et al. (2009), *CFD Analysis of incompressible turbulent swirling flow through zanker plate*, Eng. Appl. Comput. Fluid. Mech., 3(4): 562-572. doi: 10.1080/19942060.2009.11015291
17. Ben Kalifa, R., et al. (2014), *Numerical and experimental study of a jet in a crossflow for different velocity ratio*, J Braz. Soc. Mech. Sci. Eng., 36(4):743-762. doi: 10.1007/s40430-014-0129-z
18. FLUENT User Manual. FLUENT (Vol.6.3). Lebanon, NH: FLUENT, Inc., 2006.
19. Fadela, N., et al. (2008), *Reynolds stress transport modeling of film cooling at the leading edge of a symmetrical turbine blade model*, Heat Transfer Eng., 29(11):950-960. doi: 10.1080/01457630802186064

6th SUMMER SCHOOL ON FRACTURE MECHANICS

Cracow, Poland, 13-15 September 2019

Usualy, summer schools are organised together with conferences on fracture. The Summer School in Cracow will be tightly connected with the Polish Conference on Fracture Mechanics organised by Polish Group of Fracture Mechanics (ESIS National Committee). The conference will be organised by Opole Univeristy of Technology in Hucisko from 16-19 September 2019. So if you want learn more about fracture and fatigue please stay informed.

Program

Prof. Andrzej Neimitz: *Fundamentals of linear elastic and elastic-plastic fracture mechanics I and II*
Prof. Zhiliang Zhang: *Constraints effect in fracture I and II*
Prof. Jacques Besson: *Local approach to fracture for ductile failure I and II*
Prof. Meinhard Kuna: *Numerical methods in fracture mechanics I and II*

Fees

Fee paid before June 30 is 200 €
Fee paid after June 30 is 220€ (social event not guaranteed)
Fee covers lectures according to program, 4 coffee breaks, 2 lunches, 3 dinners, social event and materials for studying.

Accomodation

We recommend for Summer School participants the AGH University of Science and Technology campus hostels. Telephone: +48 12 617 3793, e-mail: marta.staniszewska@agh.edu.pl. Using code 'Summer School on Fracture Mechanics' the price of the room should be as follows: single room 70 PLN/ day; double room 90 PLN/ day. You can also use nearby hotels.

Important Dates

April 30, 2019 - Registration of participants
June 30, 2019 - Payment deadline
Sept. 13-15, 2019 – 6th Summer School on Fracture Mechanics
Sept. 16-19, 2019 – 17th Polish Conference on Fracture Mechanics

Contact info

Jaroslaw Galkiewicz
Kielce University of Technology, Aleja Tysiaclecia Panstwa Polskiego 7, 25-314 Kielce, Poland
e-mail: summerschool2019@tu.kielce.pl or jgalka@tu.kielce.pl
Phone: +48 41 34 24 711
Cellphone: +48 502 067 707